Shale Gas Well Casing Deformation in Longwall Chain Pillars under Deep Cover – Field Measurement and Numerical Modeling

Peter Zhang, Daniel Su, Mark Van Dyke, and Heather Dougherty, NIOSH, Pittsburgh Mining Research Division
Bo Hyun Kim, NIOSH, Spokane Mining Research Division

ABSTRACT

The integrity of shale gas wells in longwall chain pillars under the influence of longwall mining is a safety concern for both coal and gas operators. Previous modeling studies of gas wells in longwall pillars have shown that a FLAC3D model can predict longwall-induced stresses and deformations in gas well casings with reasonable accuracy. The predicted casing deformations can be verified by multi-finger caliper survey. This study concerns the influence of longwall mining on eight shale gas wells in a shale gas well pad located in the chain pillars between two adjacent longwall panels under 1,030 feet of cover. FLAC3D modeling was performed to predict longwall-induced deformations in gas well casings based on site-specific mining and geological conditions. Small deformations less than 0.5 in were predicted in the intermediate casing above 600 ft depth, and very small casing deformations less than 0.15 in were predicted below 600 ft due to high abutment pressure and high frictional resistance along the weak bedding interfaces. After the first panel was mined, a 56-arm caliper survey was performed on one of the wells to measure the longwall-induced casing deformations in the intermediate casing. The predicted casing deformations were then compared with the measured deformations, which indicated that the prediction was generally in good agreement with the measurement in terms of deformation locations and magnitudes. Findings from this study provide valuable information not only for stability assessment of shale gas wells in longwall chain pillars but also for developing engineering guidelines to preserve casing integrity through adequate pillar and casing design.

INTRODUCTION

Gas wells drilled in longwall pillars are influenced by longwall mining. Due to longwall-induced subsurface ground movements, the gas wells in the vicinity of longwall panels are subjected to longwall-induced stresses and deformations. Excessive stresses and deformations that occur at certain locations could lead to a casing breach. More safety concerns have been raised in unconventional shale gas wells in the presumption that the casing breach could allow high-pressure gas to leak into the mine, potentially causing a fire and explosion. Over the past decade, more than 1,500 shale gas wells have been drilled in the current and future reserves of the Pittsburgh coal seam. The impact of longwall mining on these shale gas wells will have to be evaluated as future longwall panels are mined. Therefore, it is important to quantify longwall-induced subsurface movements and casing deformations and to develop reliable models to assess the stability of shale gas wells in longwall pillars.

Longwall-induced subsurface movements and casing deformations have been studied by Su (2016, 2017), Su et al. (2018, 2019), Scovazzo (2018), Zhang et al. (2019), and Zhang and Su (2021). Instrumentation and numerical modeling were used in these studies to help understand overburden movements and casing deformations over longwall pillars. One comprehensive instrumentation study was conducted in 2013 and 2014 in a southwestern Pennsylvania coal mine under shallow cover of 604 ft by CONSOL Energy, the Marcellus Shale Coalition, and the Pennsylvania Coal Association to evaluate the effect of subsurface strata deformations on the gas well casings above the mining horizon. This study was the first instrumented study for gas well stability in longwall chain pillars, and detailed descriptions of the study site and data analysis were presented by Su (2016 and 2017) and Scovazzo (2018). Su (2016 and 2017) led the field instrumentation and measurements and conducted finite element modeling of the test wells using ABAQUS software. The study site was selected over a Pittsburgh coal seam longwall mine, which extracted 1,500-ft-wide longwall panels under about 600 feet of cover. Scovazzo (2018) presented the findings from the caliper survey. The caliper survey employing a 60-arm caliper tool was conducted on all test wells after the completion of each longwall panel. The caliper survey showed that the maximum horizontal displacement in all four test wells occurred at a depth of around 390 ft at the same location. The key findings from this instrumentation study summarized by Scovazzo (2018) include: (1) casing deformation is identified in two settings: at the weak/strong rock contacts and within the Pittsburgh coal seam; (2) casing deformation is in response to ground movement occurring at weak/strong rock contacts and is above the well intersection with the angle of draw; (3) the most significant movement is found at the weak/strong rock contact on top of Limestone D with horizontal movements in all the four test wells from 2.0 in to 5.5 in.

Along with the instrumentation study, Su (2017), using the calibrated ABAQUS model, investigated the effect of overburden depth and casing and cementing alternatives on the longwall-induced stresses and deformations in gas well casings. He found that, under deep cover, smaller lateral strata deformation is present in the overburden above the mining horizon, but higher pressure and deformation are present at and below the coal seam. He illustrated that leaving the intermediate and production casings uncemented from 50 feet below the seam to the surface can effectively uncouple the ground and the casings, making the two inside casings free from the influence of longwall-induced deformations.

The comprehensively instrumented gas well study case described above was also modeled by Zhang and Su (2021) using FLAC3D modeling to further investigate how geological factors can influence the stability of shale gas wells in longwall chain pillars under shallow cover. The modeling study concluded that horizontal movements over longwall chain pillars are also affected by coal seam and overburden dip as well as friction coefficients at interfaces. With a one degree of dip away from chain pillars, about one centimeter of additional maximum horizontal displacement could be induced along the gas well. High horizontal movement can occur when claystone interfaces are wet and the frictional coefficient is low. The comparison between the predicted and measured horizontal movements along the test well casings showed that the frictional coefficient at the interfaces along a saturated claystone layer could be as low as 0.05.

Another instrumentation study on gas wells in longwall chain pillars under shallow cover was conducted by Su et. al. (2019). The study site was located over a southwestern Pennsylvania coal mine employing 1,500-foot-wide longwall panels to extract coal from the Pittsburgh seam under 482 feet depth. The longwall panels were developed by a three-entry longwall gate-road system of 60-ft × 125-ft centers. The study by Su et al. (2019) confirmed that under shallow cover, especially under the influence of a major stream valley, longwall-induced subsurface deformations are much higher than those detected under deep cover.

In addition to the instrumentation studies under shallow cover, a deep-cover instrumentation study was conducted by Su et al. (2018). The longwalls extracted 1,500-ft-wide panels under 1,185 feet of cover in the Pittsburgh seam. One 650-ft-deep in-place inclinometer monitoring well was drilled and installed over a 150-ft by 275-ft centers abutment pillar. The study confirmed that under deeper cover, longwall-induced subsurface deformations are smaller than those observed under shallow cover, although longwall-induced vertical stress will be higher at and below the coal seam level.

To further investigate how deep cover affects longwall-induced shale gas well integrity, a recent study was conducted by researchers from the National Institute for Occupational Safety and Health (NIOSH) on actual shale gas wells in longwall chain pillars under deep cover. This study concerns the influence of longwall mining on eight shale gas wells in a shale gas well pad located in the chain pillars between two adjacent longwall panels under an overburden depth of 1,030 ft. FLAC3D modeling was performed to predict longwall-induced casing deformations in one of the gas wells based on site-specific mining and geological conditions. A 56-arm caliper survey was performed on one of the wells to measure the longwall-induced intermediate casing deformations after first panel mining. The predicted casing deformations were compared with the measured deformations to verify the modeling results. The established model was then used to analyze how deep cover affects longwall-induced casing deformations.

MINING AND GEOLOGICAL CONDITIONS AT THE STUDY SITE

The study site consists of a shale gas well pad with eight shale gas wells located in the chain pillars between two adjacent longwall panels in the Pittsburgh seam. Figure 1 shows the panel layout and shale gas well pad location. The longwall panels were developed with a three-entry system with a total chain pillar width of 220 ft center-to-center. The longwall panels are 1,573 ft wide with a mining height of 7 ft. Eight shale gas wells are located around the center of an abutment pillar of 150 ft wide rib-to-rib. The overburden depth at the well pad is 1,030 ft. One gas well, which is shown in the figure as the second one from the right along the north, was surveyed with a 56-arm caliper for casing deformations. The setback distance of the surveyed gas well is 108 ft to the current (first) longwall gob. The current longwall panel has mined past the gas well pad.

The gas well pad is located near the top of the hills. Figure 2 shows the surface topography around the gas well pad. The elevation contour lines show that the surface at the well pad dips towards a valley on the northeast side. The

elevation difference is about 150 ft between the well pad and the bottom of the valley. As surface topography has influence in surface and subsurface ground movements, it is considered in the FLAC3D model.

The overburden geology at the gas well site is determined by correlating the core log from the nearest corehole about 1,000 ft away from the well pad, and the gamma log from a gas well about 500 ft from the well pad. The locations of both the core hole and the gamma logged gas well are shown in Figure 2. Based on the core log, the overburden in the area consists of shale, sandyshale, claystone, limestone, and sandstone. Figure 3 shows gamma logs and weak interface locations. Weak interfaces include weak claystone layers and coal seams. The weak claystone layers are identified from the gamma logs, and the coal seams are identified from the core log. Three main coal seams are present above the Pittsburgh seam. The weak interfaces represent the weak bedding between a weak layer and a relatively strong massive strata and are implemented in the FLAC3D model.

FLAC3D MODEL FOR GAS WELLS IN LONGWALL CHAIN PILLARS

To quantitatively evaluate the influence of longwall mining on shale gas wells in longwall pillars, NIOSH researchers have developed FLAC3D modeling techniques to calculate longwall-induced stresses and deformations (Zhang and Su, 2021, Su et al. (2018, 2019), Zhang et al., 2019, and Tulu et al., 2017). In this study, a FLAC3D model (Itasca, 2017) was set up based on the geological conditions and longwall mining layouts around the shale gas well pad. Figure 4 shows the cross-sectional view of the FLAC3D model. The model included overburden from the Pittsburgh seam to the surface. The overburden lithology was based on the lithology from the nearest corehole about 1,000 ft from the gas well pad. Table 1 shows the rock properties used in the model. The weak bedding interface locations were based on the gamma logs from the nearest gas well about 500 ft from the well pad. Surface slope over the longwall panel was also modeled. The longwall caving zone was modeled by strain-hardening material implemented by the "FISH" scripting language available in FLAC3D. The overburden strata above the caving zone were modeled with ubiquitous joint materials, and the coal seam, immediate roof, and floor were modeled with Mohr-Coulomb materials. In-situ horizontal stresses were applied in the model with a maximum horizontal stress of three times the vertical stress along the panel and a minimum horizontal stress of two times the vertical stress across the panel.

The gas well casings were modeled according to their construction and specifications. Only the caliper surveyed gas well was modeled. Figure 5 shows the construction of the gas well in the model and casing specifications. As the casings are subjected to horizontal movements towards the gob, only half of the casings were implemented in the model to take account of symmetry along the panel's longitudinal direction. At the gas well pad, three casings were originally installed past the Pittsburgh coal seam. As the production casing was uncemented and was pulled out before the longwall face mined by, the production casing was not included in the model. Both surface casing and intermediate casing were fully cemented from the surface through the Pittsburgh seam horizon. The steel casings were modeled with von Mises material, and the cement fillings were modeled with Mohr-Coulomb material. The casings were installed in the model before the longwall gate entries were developed. Table 2 shows the input parameters for shale gas well casings in the model.

The FLAC3D model was set up for the study site based on site-specific mining and geologic conditions and was verified with surface subsidence and pillar pressure as their measurements in similar mining conditions are available for comparison. Figure 6 shows predicted and measured final surface subsidence across the gas well and longwall panel after the first panel is completed. The predicted final subsidence curve is almost flat around the panel center but is asymmetrical due to the presence of surface slope above the panel. The model predicts a maximum subsidence of about 4.3–4.4 ft around the panel center. At the gas well location, the predicted surface subsidence is about 2.5 in after first panel mining. The measured surface subsidence for comparison is from a subsidence survey on an adjacent longwall panel with similar mining conditions and overburden depth. By comparison, the predicted surface subsidence shows a reasonable agreement with the measured subsidence in both subsidence profile and maximum subsidence.

The predicted vertical stress distribution across the chain pillars at the coal seam horizon is shown in Figure 7. At the coal seam horizon, the gas well is mainly influenced by the longwall-induced vertical stress in the coal pillar near the well. The predicted pillar pressure increase is about 400 psi after first panel mining. In comparison with the measured pillar pressure increase under similar overburden depth by Su et al. (2018), the model reasonably predicts the longwall-induced vertical stress around the chain pillars.

LONGWALL-INDUCED STRESSES AND DEFORMATIONS IN THE INTERMEDIATE CASING

In this study, the verified model was used to predict casing stresses and deformations, and the predicted casing deformations were compared with the measured casing deformations. The deformations in the intermediate casing were measured by the 56-arm caliper after the current (first) panel mined-by the well pad. The caliper survey measures the inside diameter along the casing and provides indications about the locations and magnitudes of casing deformation.

The predicted horizontal displacement along the intermediate casing is shown in Figure 8. With first panel mining, the casing moves towards the current panel. At the surface, the casing moves about 2.1 in towards the gob. In the subsurface, the casing is also subjected to relative horizontal displacements or shear displacements at interface locations. Casing deformations are caused by relative horizontal displacements along strong/weak rock interfaces. Based on the horizontal displacement curve, the casing deformations are predicted at the locations shown in Figure 8. In this case, the casing deformations are small since the relative horizontal displacements at the interfaces are small. The horizontal displacement curve also indicates that the relative horizontal displacements are even smaller below a 600-ft depth. The small relative horizontal displacement and casing deformation under deep cover can be attributed to high frictional resistance along the interfaces under high abutment pressure.

The casing deformations were measured by 56-arm caliper survey after first panel mining. Figure 9 shows the measured minimum diameters along the intermediate casing and diameter changes at the deformation locations. The nominal casing inside diameter for the 9-5/8-in 40# casing is 8.835 in. This figure shows that the casing diameters are reduced at deformation locations. Casing deformations are detected at 10 locations below the surface. All the measured deformations are less than 0.5 in. Figure 9 also shows that very small deformations occur below 600 ft depth. The casing deformation locations are compared with the overburden geology at the gas well pad as shown in Figure 3. It is apparent that all the casing deformations occur at the weak claystone or coal interfaces. Figure 10 shows the 3D view of the casing deformation at 191-ft depth. According to the gamma logs, the deformation occurred at a claystone interface. As the casing deformation is induced by shear displacement at the claystone interface, the extent of the deformation along the casing is restricted within about 6 in to 1 foot from the interface.

The comparison between predicted and measured casing deformations after first panel mining is summarized in Table 3. The predicted relative displacement at different depths is obtained from the horizontal displacement along the intermediate casing in Figure 8. The minimum casing diameter change is estimated from the predicted relative displacement multiplied by a factor of 1.4. This factor is determined according to the field measurement of casing deformations under shear displacement (Zhang, et al. 2022). From the caliper survey, the casing becomes ovalized after being deformed. The orientation of the deformed casing along the minimum diameter tends to be perpendicular to the longwall mining direction. Under the shear displacement at an interface across the longwall mining direction, the casing deforms on two sides opposite to each other. One side is the active side which is subjected to active force, and the other side is the reactive side. The deformation on the active side generally matches the relative horizontal displacement along the interface. The deformation on the reactive side is less than that at the active side. Based on the field measurement of a test well using a 60-arm caliper survey, the deformation at the reactive side is about 40% of the amount at the active side. The deformation at each side causes a radius change in the casing. The sum of the radius changes is the minimum diameter change which can be estimated at about 1.4 times the predicted horizontal relative displacement.

As shown in Table 3, the predicted minimum casing diameter changes are in reasonable agreement with the measured minimum casing diameter changes in terms of deformation level and location. Since relative horizontal displacement at an interface is affected by many factors such as overburden depth, surface topography, interface friction, thickness of the beds above and below the interface, and distance from the mining horizon, it is difficult to predict casing deformations with a high degree of accuracy. But for the purpose of gas well stability assessment, it is more important to know at what horizon casing could potentially deform and to what level the deformation could reach. Figure 11 shows a visual view of predicted deformation locations and caliper-detected deformation locations. The predicted deformation locations are generally in good agreement with the measured deformation locations.

Casing deformations are an indication of high stresses in the casing, and casing yielding can be predicted by von Mises stress. The von Mises stress represents a combination of all the longwall-induced stress components such as vertical, horizontal, and shear stresses. Figure 12 shows the von Mises stress and deformation locations in the

intermediate casing. This figure shows that casing deformations occur at locations with high von Mises stress. The high von Mises locations above the coal seam are generally at the weak interfaces. With small deformations, no yielding occurs in the casing. At the coal seam horizon, the predicted von Mises stress is 44,400 psi, which is less than the casing yield strength of 50,000 psi. Although the von Mises stress is relatively high at the coal seam level, the casing remains elastic after first panel mining.

THE EFFECT OF DEEP COVER ON OVERBURDEN MOVEMENTS AND CASING DEFORMATIONS

With the established FLAC3D model, the effect of deep cover on overburden movements and casing deformations was further investigated. The overburden movements are affected by many factors including mining conditions, surface features, and site-specific overburden geology. Casing deformations are caused by longwall-induced overburden movements over chain pillars which are transferred to gas well casings. Overburden depth affects the location and the level of deformation to be induced in the casing. Under shallow cover, relatively large horizontal displacements and casing deformations have been observed in the gas well casing above the mining horizon (Su, 2016, 2017; Scovazzo, 2018; Zhang and Su, 2021). Under deep cover, the current study and a previous study (Su et al., 2018) both indicated that the casing deformations are relatively small above the coal seam. The effect of overburden depth on casing deformation can be better explained by the modeling results.

The effect of overburden depth on shear displacements along interfaces was investigated with the model. The casing deformations above the coal seam are largely caused by shear movements along interfaces. The shear displacements along interfaces can be obtained from the model. Figure 13 shows the shear displacements along the interfaces at different depths over the chain pillars. The locations of depths in the figure are chosen as the interface locations where casing deformations were detected. This figure shows that shear displacement at an interface horizon changes with its relative location to the edge of the gob and its distance above the coal seam. Along an interface horizon, peak shear displacement occurs over the gob and quickly reduces over the chain pillars. The peak value and the rate of reduction depend on interface friction and the thickness of strong strata below and above the interface. In this case, the shear displacements at four interface horizons peak at about 2–6 in over the gob and reduces to less than 0.5 at the gas well 108 ft from the gob. Therefore, the farther the gas well is located from the longwall gob, the smaller the shear displacement is. This figure also shows that the location of the peak shear displacement changes with the distance of the interface to the coal seam. With the effect of subsurface subsidence, the peak shear displacement tends to be away from the chain pillars for the interfaces at shallower depths. As the figure shows, the peak shear displacement at the 191-ft depth is about 50 ft further away from the gob edge than the peak shear displacement at the 603-ft depth. With increasing depth, the peak shear displacement gets closer to the gas well, but its magnitude becomes lower. This can be one reason why the casing deformations are small in this studied case with an overburden depth of 1,030 ft.

The effect of abutment pressure on the frictional resistance along interfaces is also examined with the model. Both prediction and measurement show small casing deformations below a 600-ft depth. This can be attributed to high frictional resistance along the interfaces due to high abutment pressure on the interfaces at the deeper depth. Figure 14 shows the longwall-induced vertical stress at different depths above the chain pillars 10 ft and 50 ft from the gob. In-situ vertical stress at different depths is also plotted for comparison. With the influence of the longwall gob, the vertical pressure over the chain pillars increases at a greater rate at deeper depths. At a 600-ft depth, the vertical pressure is about 900 psi at a distance 50 ft from the gob, about 150 psi above the overburden pressure. At a depth of 900 ft, the vertical pressure increases to 1,400 psi at the same distance from the gob, about 400 psi above the overburden pressure. As the longwall-induced vertical pressure at a deeper depth is higher, the frictional force along the interfaces is also higher. At a greater depth, the high frictional force on the interfaces contributes to the reduction of shear displacements along the interface. Therefore, the longwall-induced casing deformations above the coal seam horizon tend to be smaller under deep cover than under shallow cover.

CONCLUSIONS

In this study, a shale gas well in the chain pillars between two adjacent longwall panels was modeled using the FLAC3D modeling technique for longwall-induced stresses and deformations in the intermediate casing. The predicted casing deformations were compared with the measured deformations from a multi-finger caliper survey. Important conclusions from this study include:

- With first panel mining, casing deformations in gas wells in longwall chain pillars could occur above the coal seam horizon, and the deformation is due primarily to relative horizontal displacements along weak claystone/coal interfaces.
- A FLAC3D model can predict longwall-induced stresses and deformations in gas well casings. The prediction is generally in good agreement with field measurement in terms of deformation locations and magnitudes.
- Under deep cover, casing deformations are small, and the small deformation can be attributed to smaller subsurface relative horizontal movements at the gas well due to high longwall-induced abutment pressure and associated high frictional resistance along weak interfaces.

DISCLAIMER

The findings and conclusions in this report are those of the author(s) and do not necessarily represent the official position of the National Institute for Occupational Safety and Health, Centers for Disease Control and Prevention (CDC). Mention of any company or product does not constitute endorsement by NIOSH.

REFERENCES

ITASCA Consulting Group, Inc. 2017. FLAC-3D, Version 6.0, User's Guide.

Scovazzo, V. 2018. Mining effects on gas and oil wells pad NV-35 field experiment field monitoring. In *Proceedings of the 37th International Conference on Ground Control in Mining*. Morgantown, WV: West Virginia University, pp. 30–43.

Su, D.W.H., Zhang, P., Dougherty, H., Van Dyke, M., Minoski, T., Schatzel, S., Gangrade, V., Watkins, E., Addis, J., and Hollerich, C. 2019. Longwall-induced subsurface deformations and permeability changes – Shale gas well casing integrity implication. In *Proceedings of the 38th International Conference on Ground Control in Mining*. Morgantown, WV: West Virginia University, pp. 49–59.

Su, D.W.H., Zhang, P., Van Dyke, M., and Minoski, T. 2018. Effects of longwall-induced subsurface deformations on shale gas well casing stability under deep covers. In *Proceedings of the 37th International Conference on Ground Control in Mining*. Morgantown, WV: West Virginia University, pp. 63–70.

Su, D.W.H. 2017. Effects of longwall-induced subsurface deformations on the mechanical integrity of shale gas wells drilled over a longwall abutment pillar. *2017 SME Annual Meeting*, Feb.19-22, 2017, Denver, CO. Preprint 17-051, pp. 1-6.

Su, D.W.H. 2016. Effects of longwall-induced stress and deformation on the stability and mechanical integrity of shale gas wells drilled through a longwall abutment pillar. In *Proceedings of the 35th International Conference on Ground Control in Mining*. Morgantown, West Virginia, pp. 119–125.

Tulu, I.B., Esterhuizen, G.S., Mohamed, K.M., Klemetti, T.M. 2017. Verification of a calibrated longwall model with field measurements. In *Proceedings of the 51st US Rock Mechanics/Geomechanics Symposium*, 25–28 June 2017. San Francisco, California.

Zhang, P., Su, D., Kim, B., and Midler, E., 2022. Comparison of measured and modeled casing deformations of a test well in a longwall abutment pillar. In *Proceedings of the 56th US Rock Mechanics/Geomechanics Symposium*, 27–29 June 2022. Santa Fe, New Mexico.

Zhang, P. and Su, D., 2021. FLAC3D modeling evaluation of the comprehensive NV-35 gas well pillar study. In *Proceedings of the 55th US Rock Mechanics/Geomechanics Symposium*, 20–23 June 2021. Texas.

Zhang, P., Dougherty, H., Su, D., and Trackemas, J. 2019. Influence of longwall mining on the stability of gas wells in chain pillars. In *Proceedings of the 38th International Conference on Ground Control in Mining*, Morgantown, West Virginia, pp. 38–48.

Table 1. Rock properties used in the model

Rock Type	Young's Modulus, psi	Poisson's Ratio	Cohesion, psi	Internal Friction Angle, degrees	Tensional Strength, psi
coal	3.00×10^5	0.30	270	28	40
claystone	4.20×10^5	0.30	270	28	40
shale	1.68×10^6	0.25	1,700	35	650
sandyshale	1.68×10^6	0.25	1,700	35	650
sandstone	1.68×10^6	0.25	2,600	35	1,000
limestone	2.52×10^6	0.22	2,300	35	885
shaley limestone	2.52×10^6	0.22	2,100	38	850
shaley sandstone	2.18×10^6	0.22	1,700	38	700
siltyshale	1.68×10^6	0.25	1,700	32	600

Table 2. Input parameters for shale gas well casings in the model

Casing Type	Outside Diameter, in	Wall Thickness, in	Young's Modulus, psi	Poisson's Ratio	Yield Strength, psi
Surface casing	13.375	0.380	2.9×10^7	0.3	55,000
Intermediate casing	9.625	0.395	2.9×10^7	0.3	50,000
Production casing	5.500	0.361	2.9×10^7	0.3	110,000

Table 3. Comparison between predicted and measured casing deformations after first panel mining

Depth Below Surface, ft	Predicted Relative Displacement, in	Estimated Minimum Diameter Change, in	Measured Minimum Diameter Change, in
191	0.30	0.42	0.43
253	0.25	0.35	0.2
325	0.10	0.14	0.07
519	0.08	0.11	0.45
582	0.00	0.00	0.16
603	0.21	0.29	0.5
640	0.10	0.14	0.05
720	0.02	0.03	0.04
850	0.03	0.04	0.14
914	0.02	0.03	0.09

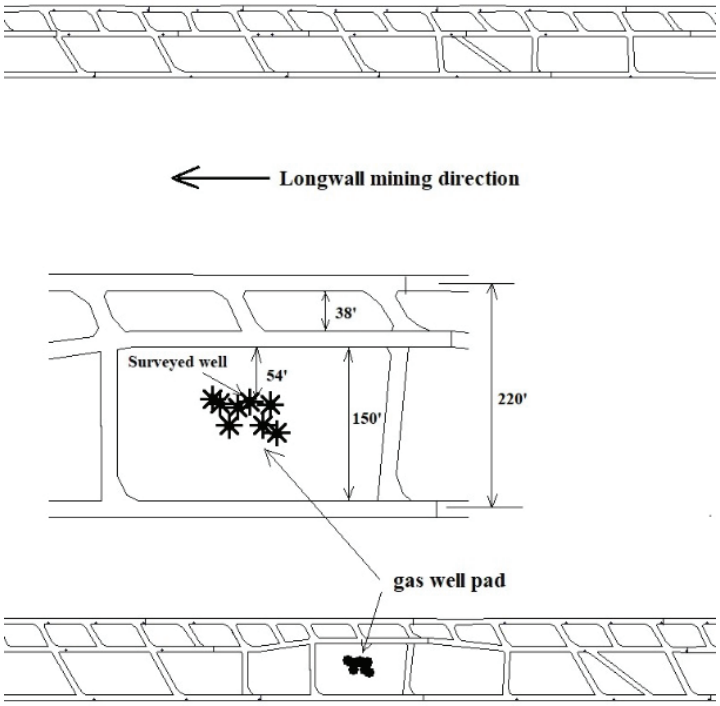

Figure 1. Longwall panel layout and shale gas well pad location.

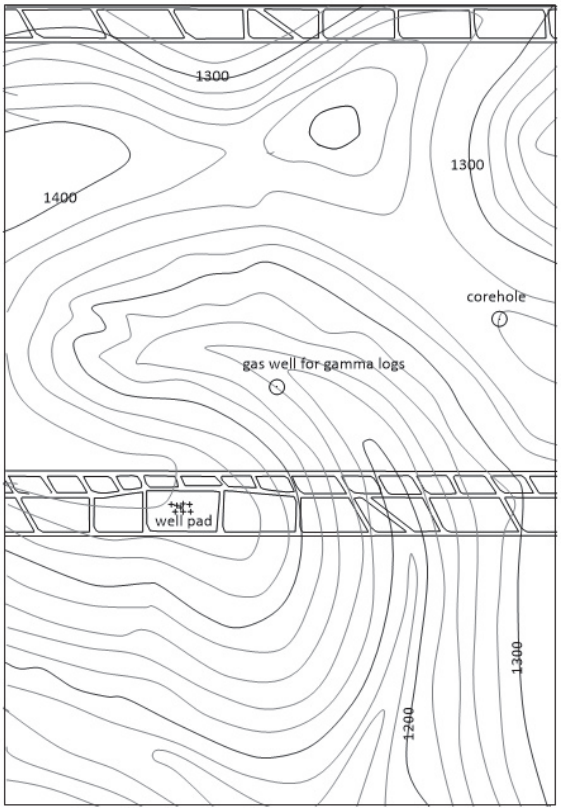

Figure 2. Surface topography around the gas well pad.

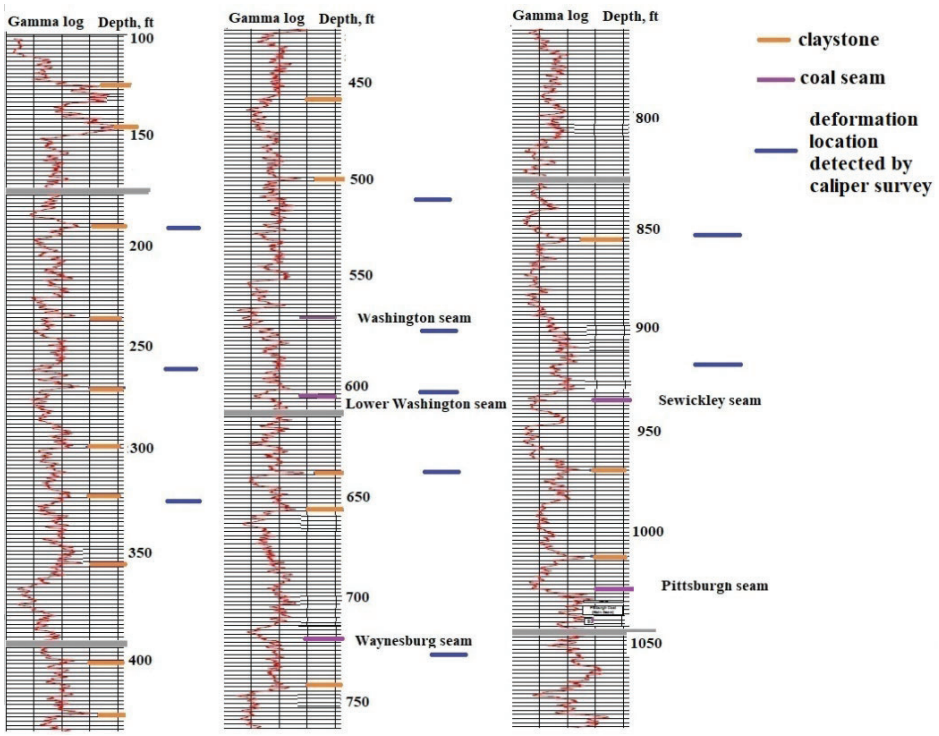

Figure 3. Gamma logs and weak interface locations.

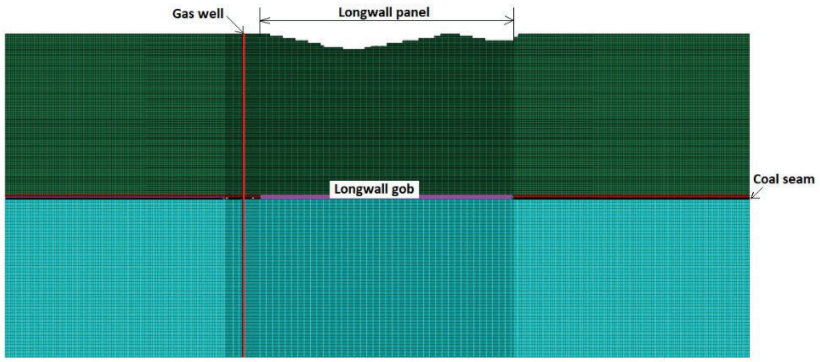

Figure 4. Cross-sectional view of the FLAC3D model.

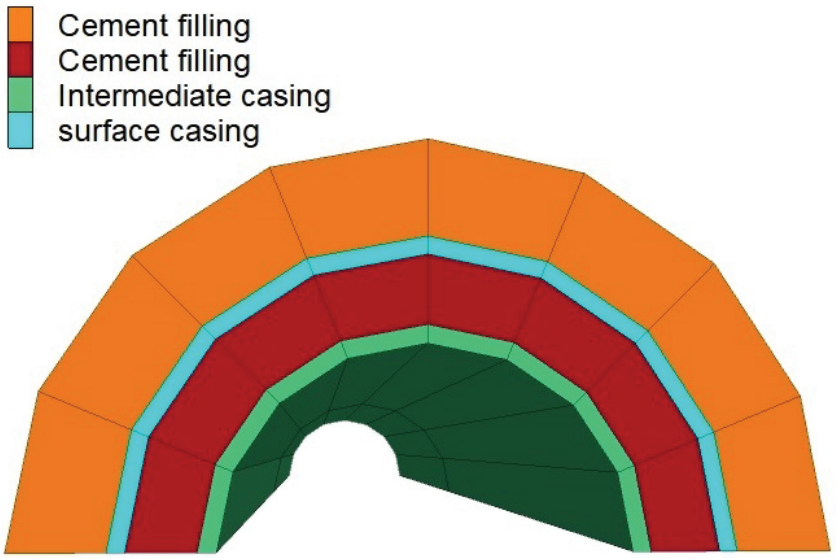

Gas well casing information

Casing	Size	Weight	Grade	TOC
Surface	13.375"	54.5#	J-55	Surface
Intermediate	9.625"	40#	MC-50	Surface

Figure 5. Gas well casing construction in the model and casing specifications.

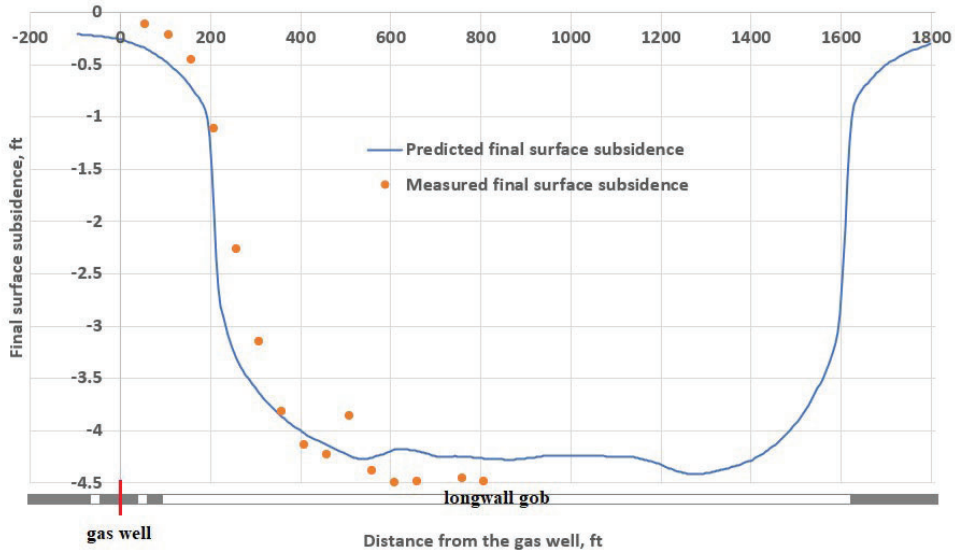

Figure 6. Predicted and measured final surface subsidence across the gas well and longwall panel after the first panel is completed.

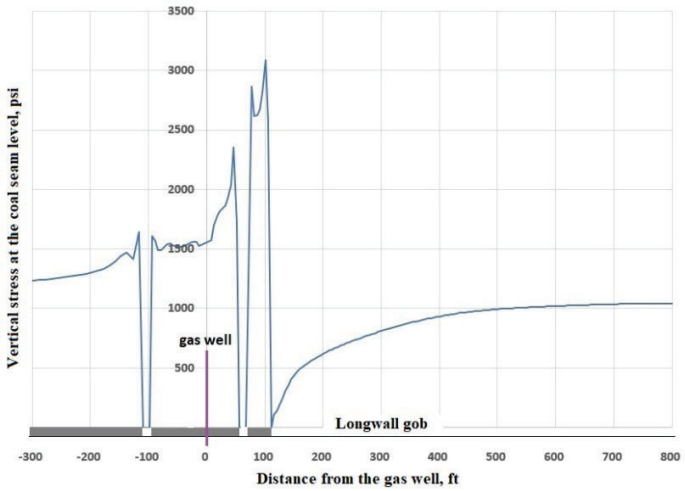

Figure 7. Predicted vertical stress distribution across the chain pillars at the coal seam horizon.

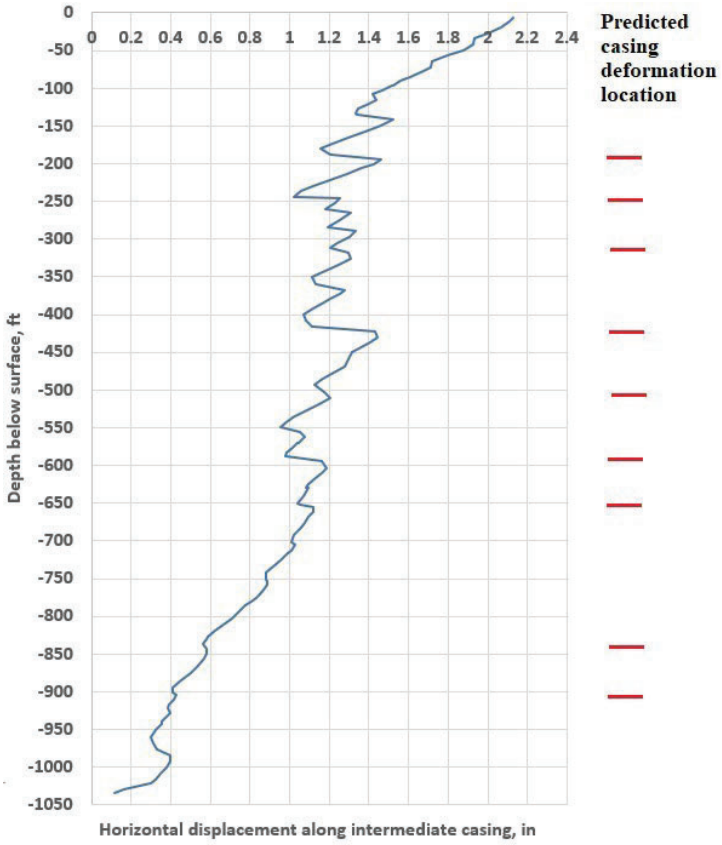

Figure 8. Predicted horizontal displacement along intermediate casing.

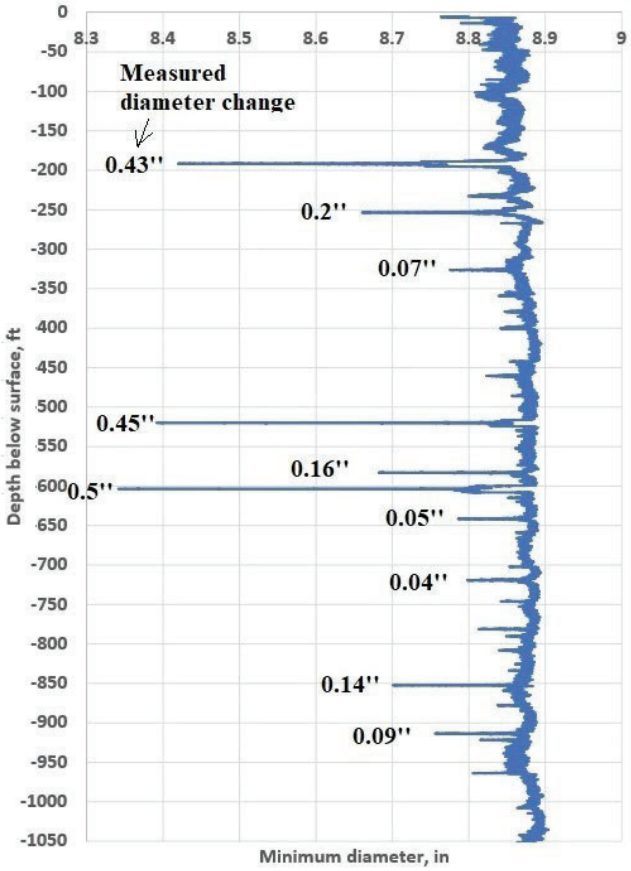

Figure 9. Measured minimum diameters along the intermediate casing.

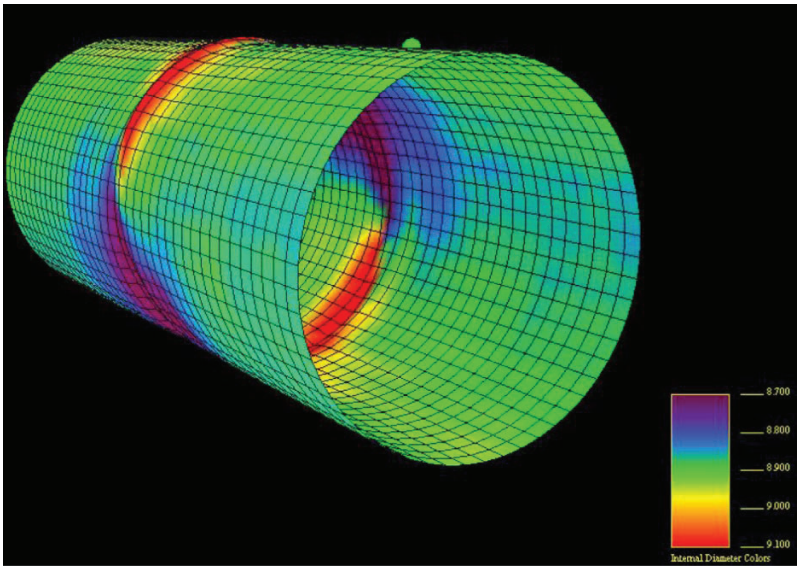

Figure 10. 3D view of the casing deformation at 191-ft depth.

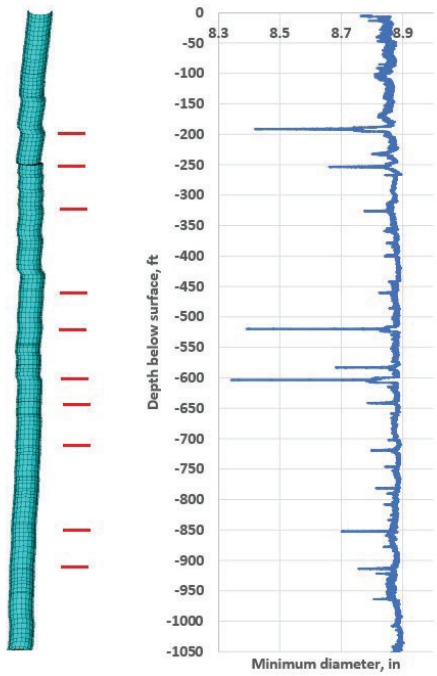

Figure 11. Comparison of predicted deformations and caliper-detected deformations.

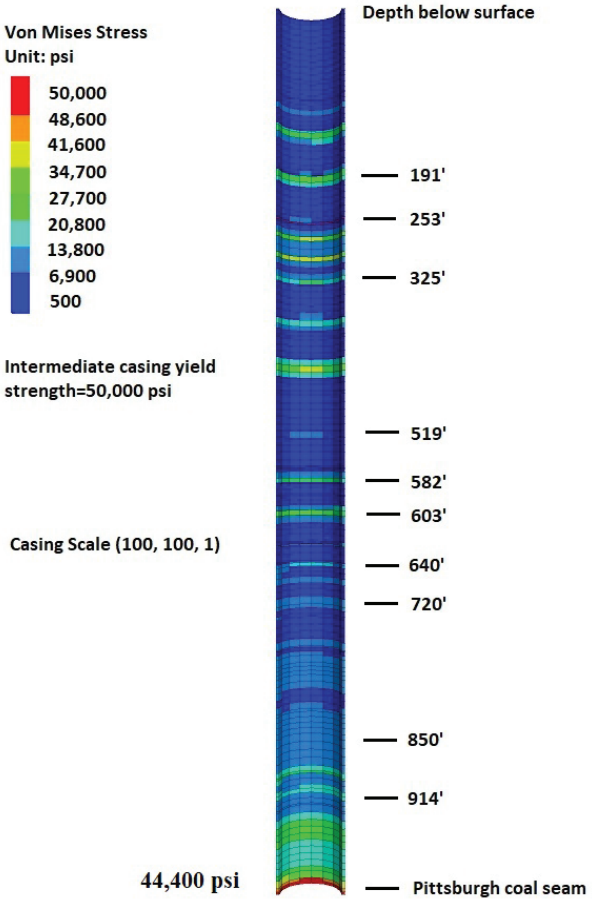

Figure 12. Von Mises stress and deformation locations in the intermediate casing.

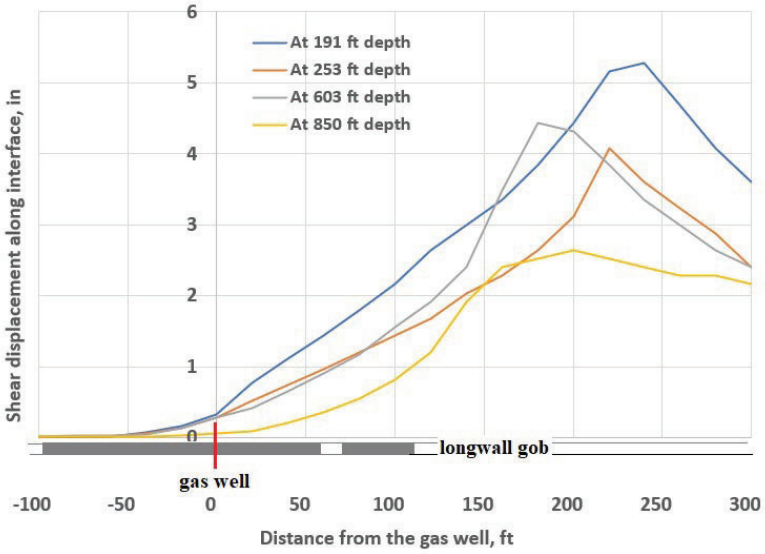

Figure 13. Shear displacement along the interfaces at different depths over the chain pillars.

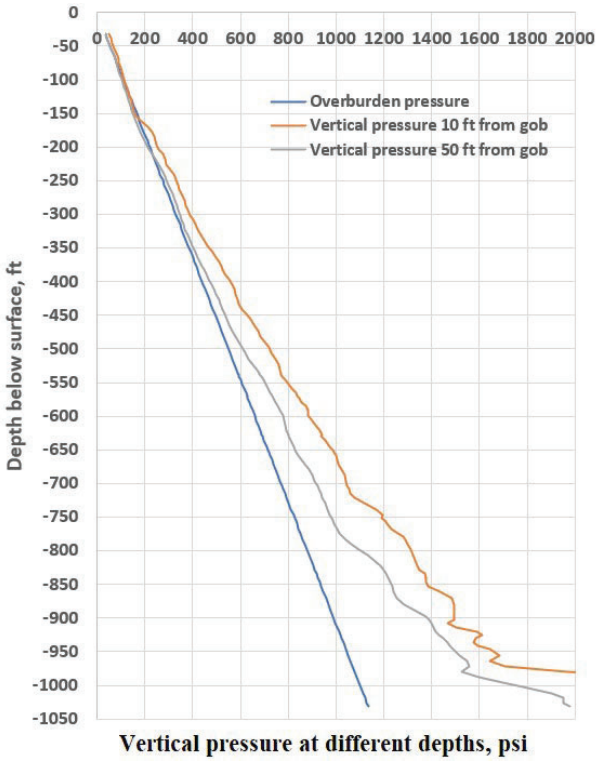

Figure 14. Longwall-induced vertical pressure above the chain pillars.